Protoplasma (2023) 260:571–587
https://doi.org/10.1007/s00709-022-01802-w

ORIGINAL ARTICLE

Anther development in *Brachiaria brizantha* (syn. *Urochloa brizantha*) and perspective for microspore in vitro culture

Andréa D. Koehler[1,2] · Mônica L. Rossi[1] · Vera T. C. Carneiro[2] · Glaucia B. Cabral[2] · Adriana P. Martinelli[1] · Diva M. A. Dusi[2]

Received: 8 April 2022 / Accepted: 31 July 2022 / Published online: 10 August 2022

Abstract

Brachiaria, a genus from the Poaceae family, is largely cultivated as forage in Brazil. Among the most cultivated varieties of *Brachiaria* spp., *B. brizantha* cv. Marandu (syn. *Urochloa brizantha*) is of great agronomical importance due to the large areas cultivated with this species. This cultivar is apomictic and tetraploid. Sexual diploid genotype is available for this species. The difference in levels of ploidy among sexual and apomictic plants contributes to hindering *Brachiaria* breeding programs. The induction of haploids and double haploids is of great interest for the generation of new genotypes with potential use in intraspecific crosses. A key factor for the success of this technique is identifying adequate microspore developmental stages for efficient embryogenesis induction. Knowledge of the morphological changes during microsporogenesis and microgametogenesis and sporophytic tissues composing the anther is critical for identifying the stages in which microspores present a higher potential for embryogenic callus and somatic embryo through in vitro culture. In this work, morphological markers were associated with anther and pollen grain developmental stages, through histological analysis. Anther development was divided into 11 stages using morphological and cytological characteristics, from anther with archesporial cells to anther dehiscence. The morphological characteristics of each stage are presented. In addition, the response of stage 8 anthers to in vitro culture indicates microspores initiating somatic embryogenic pathway.

Keywords In vitro microspore embryogenesis · Male gametophyte · Microgametogenesis · Microsporogenesis · Poaceae · Ultrastructure

Introduction

Brachiaria is an economically important genus of the family Poaceae, a forage grass cultivated in tropical countries, especially in Brazil, where breeding programs aim to obtain better forage quality, resistance to pests and diseases, and high seed production, among other traits (Valle et al. 2009).

Brachiaria brizantha (syn. *Urochloa brizantha*) is one of the species with great importance for breeding purposes. In this and other species, such as *B. decumbens* (syn. *U. decumbens*) the cultivated plants are tetraploids and reproduce by apomixis. Apomixis is an asexual mode of reproduction through seeds (Nogler 1984), which generate plants that are clones of the mother plant. As a consequence of apomixis, cultivated areas with apomictic plants of *B. brizantha* or *B. decumbens* are wide monocultures, implying potential economic and environmental risks (Dusi 2001). Sexual diploid noncultivated genotypes are available for both species; however, the difference in levels of ploidy among sexual and apomictic plants impairs breeding (Valle et al. 2009). Approaches to producing hybrids include interspecific and intraspecific crosses between apomicts and artificial tetraploid sexual plants (Miles and Valle 1996; Monteiro et al. 2016), followed by a selection of desired traits in the progeny.

Handling Editor: Benedikt Kost

✉ Diva M. A. Dusi
diva.dusi@embrapa.br

Adriana P. Martinelli
adriana@cena.usp.br

[1] University of Sao Paulo, CENA, Av. Centenario 303, Piracicaba, SP 13416-903, Brazil

[2] Brazilian Agricultural Research Corporation (Embrapa), Embrapa Genetic Resources and Biotechnology, Cx.Postal 02372, Brasilia, DF 70.770-917, Brazil

In *Brachiaria* spp., apomixis occurs by apospory with pseudogamy, meaning—the fertilization of the central cell by the male reproductive cell is necessary for endosperm development (Alves et al. 2001; Dusi 2001). *Brachiaria* spp. apomictic plants produce viable pollen grains (Dusi et al. 2010; Dusi and Willemse 1999a). In some genotypes of *B. decumbens*, pollen grains follow the same pattern of development in sexual and apomictic plants, resulting in the production of viable pollen grains, varying in the degree of abortion of microspores and mature pollen grains, which is higher in apomictics (Dusi et al. 2010; Dusi and Willemse 1999a). In another genotype, correspondent to the apomictic *B. decumbens* cv. Basilisk, sterile pollen grains resulted from abnormal pollen mitoses (Junqueira Filho et al. 2003). Synchrony among male and female development was observed (Dusi and Willemse 1999a), thus anther and pistil morphology should be a good indicator for the stage of pollen development.

The cytogenetic and morphological characterizations of microsporogenesis or microgametogenesis in diploid, tetraploid, and induced tetraploid plants of *Brachiaria* spp. (Araujo et al. 2005; Dusi et al. 2010; Dusi and Willemse 1999a; Mendes-Bonato et al. 2002, 2009; Risso-Pascotto et al. 2006) assist the selection of genotypes that produce high amounts of viable pollen that could be used as male progenitors in conventional breeding programs or for in vitro fertilization.

Haploids and doubled haploids are important sources for the generation of new genotypes with potential use in intraspecific crosses (Weyen 2021), which may contribute to the study of sexual and apomictic reproduction in *Brachiaria* spp. A key factor for the success of haploid production through in vitro culture is to identify the adequate microspore developmental stages for efficient embryogenesis induction, with morphological markers being very helpful to choose the best explant stage to be introduced in vitro. The knowledge of morphological characteristics of pistil, spikelet, and flower sizes according to stages of the ovule, embryo sac, and pollen development, has proven to be very useful for molecular and cellular studies of *Brachiaria* spp. reproduction (Alves et al. 2007; Dusi and Willemse 1999a, b; Dusi 2001; Guimarães et al. 2013; Lacerda et al. 2012; Rodrigues et al. 2003; Silveira et al. 2012; Worthington et al. 2016). Nevertheless, few reports emphasize the pollen grain development, and the detailed events during anther development are yet to be described in this genus. Histological characterization of anther and microspore/pollen grain development in *B. brizantha* will increase the possibility of application of biotechnological techniques in this forage. The objective of this work was to characterize anther development stages in *B. brizantha*, providing histological and ultrastructural details, and correlating them with morphological characteristics. *BbrizSERK* expression was found to be a marker in the process of somatic embryogenesis in *B. brizantha* (Koehler et al. 2020) in vitro culture and the possibility of using the expression of this gene as a marker to track embryogenesis inside the anther should be investigated.

The inflorescence of *Brachiaria* is a panicle with racemes that support the spikelets placed in two series on the raceme (Skerman and Riveros 1989). Each spikelet has two flowers, a male and a hermaphrodite flower (Dusi 2001; Ndikumana, 1985). Both types of flowers have three stamens each. Each anther has a connective tissue (with vascular bundle) with two thecae and four locules, and dehiscence is longitudinal. In this article, we report the histological, cytological, and ultrastructural characterization of anthers of sexual accession of *B. brizantha* and correlate the stages of development to morphological markers. In addition, we present a first impression of the response of anthers cultured in vitro using histology and the expression of *BbrizSERK* to observe the transition of microspore development to an embryogenic route.

Material and methods

Plant material

Two diploid (2n = 2x = 18) sexual accessions, *B. brizantha* BRA 002,747, and *B. decumbens* BRA 004,430, were used, from the germplasm collection of Embrapa, cultivated in the experimental field at Embrapa Genetic Resources and Biotechnology.

Structural and ultrastructural analysis of the in vivo anther development

Developmental stages were associated with the following morphological parameters: in the early stages of development, the length of spikelet or hermaphrodite flower, and in later stages, the length and coloration of anthers and pistil morphology. Pistil morphology was annotated according to Dusi and Willemse (1999a), based on the aspect of the stylodia, which in grasses constitute the so-called stigma (Heslop-Harrison 1982).

Spikelets, hermaphrodite flowers, and anthers from the hermaphrodite flowers of *B. brizantha* were collected from plants growing in the field, at different stages of development. For transmission electron microscopy (TEM), explants were fixed in a modified Karnovsky solution (2% glutaraldehyde, 2% paraformaldehyde, and 0.001 M $CaCl_2$ in 0.2 M sodium cacodylate buffer,

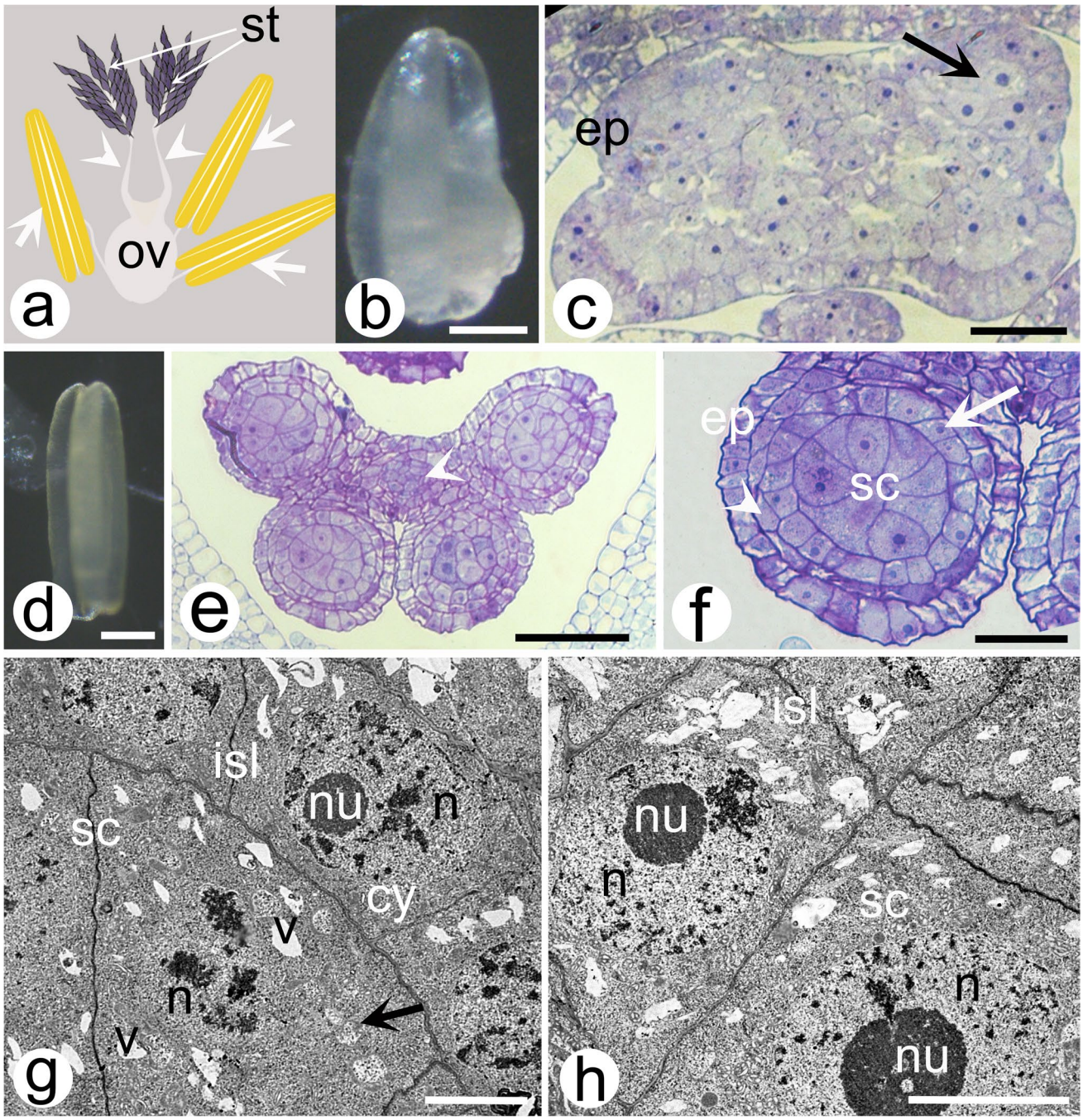

Fig. 1 Anther development in *B. brizantha*, stages 1 to 2. **b–f** LM images, **g**, **h** TEM image. **a** Schematic representation of a dissected hermaphrodite flower of *Brachiaria* showing the three anthers (arrows) and in the pistil, the ovary, the two styles (arrowhead), and the stylodia. **b** Stage 1 anther. **c** Cross-section showing epidermis and archesporial cell (arrow). **d** Anther at stage 2. **e** Cross-section showing the four locules anther with the connective tissue (arrowhead). **f** Anther in stage 2 showing epidermis, outer (arrowhead) and inner (arrow) subepidermal layers and sporogenous cells. **g**, **h** Detail of the inner subepidermal layer and sporogenous cells from anther at stage 2; the arrow points to mitochondria/plastids. Abbreviations: cn, connective tissue; ct, cuticle; cy, cytoplasm; ep, epidermis; isl, inner subepidermal layer; n, nucleus; nu, nucleolus; ov, ovary; sc, sporogenous cells; v, vacuoles. Scale bars = 0.2 mm (**b**), 25 µm (**c**), 0.2 mm (**d**), 50 µm (**e**), 20 µm (**f**), and 8 µm (**g**, **h**)

pH 7.2), for 48 h, under refrigeration and post fixed in osmium tetroxide (1% in 0.1 M sodium cacodylate buffer, pH 7.2), for 1 h, at room temperature. Samples were then dehydrated in an acetone series (30–100%) and infiltrated and embedded in Spurr's (1969) low viscosity resin (EMS, Electron Microscopy Sciences, Hatfield,

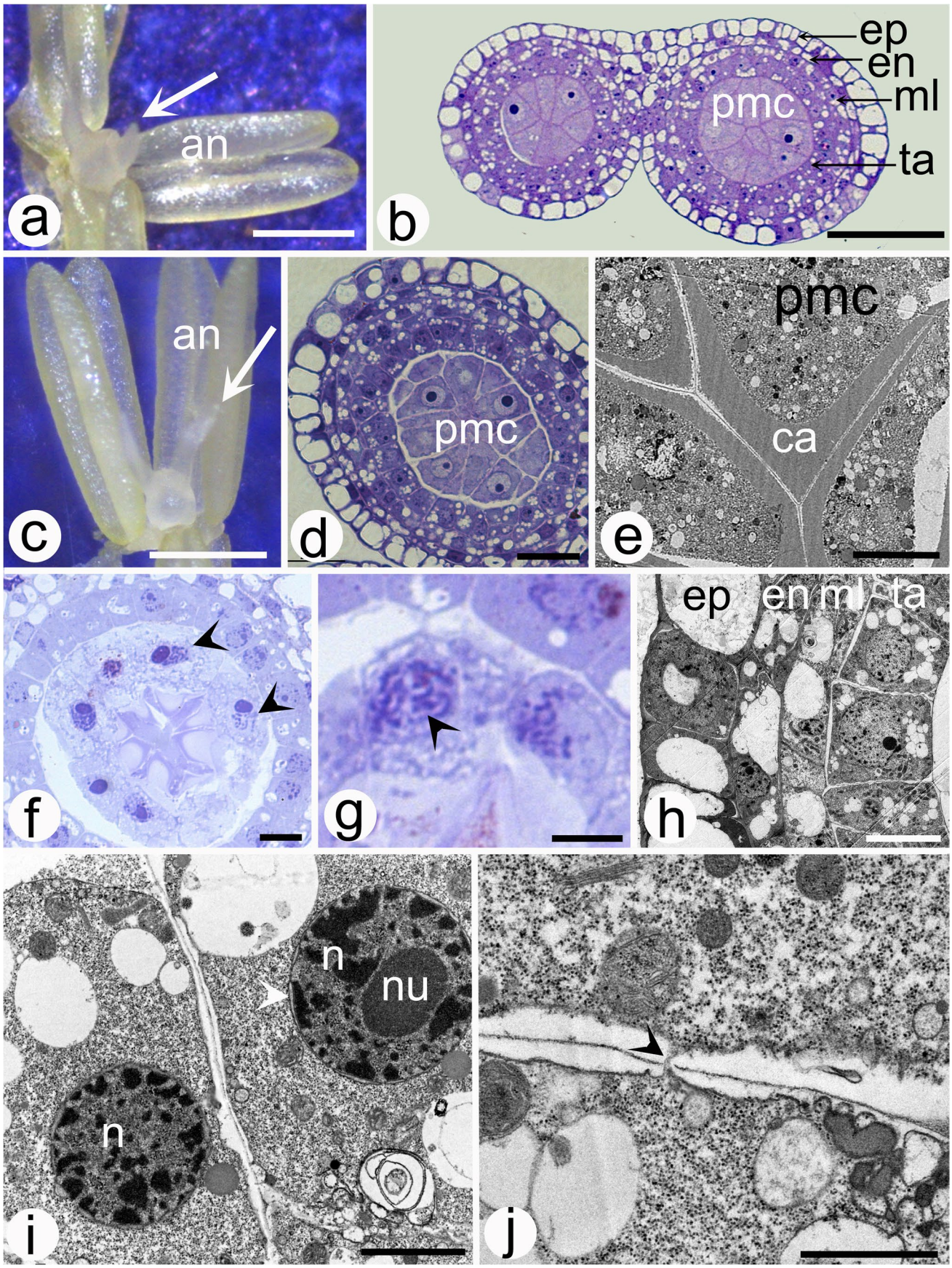
an
a
ep
en
ml
ta
pmc
b
an
c
pmc
d
pmc
ca
e
f
g
ep
en
ml
ta
h
n
nu
n
i
j

◂**Fig. 2** Anther development in *B. brizantha*, stages 3 and 4. **a–d, f–g** LM images, **e, h–j** TEM images. **a** Dissected flower with anthers at stage 3 showing the pistil with very small stylodia (arrow). **b** Anther wall formed by four layers and the pollen mother cells. **c** Dissected flower with anthers at stage 4 showing anthers and stylodium beginning to elongate. **d** Detail of an anther showing PMC. **e** Callose deposition in the inner part of the locule of the anther, surrounding pollen mother cells. **f** Meiocytes at prophase (arrowheads). **g** Meiocyte at anaphase (arrowhead). **h** Detail of the anther wall with highly vacuolated cells of epidermis, endothecium, and middle layer. **i** Detail of a tapetum cell showing a conspicuous nucleus with an evident nuclear envelope (arrowhead) and a prominent nucleolus. **j** Detail of the tapetum cells connected by plasmodesmata (arrowhead). Abbreviations: an, anther; ca, callose; en, endothecium; ep, epidermis; ml, middle layer; ov, ovary; pmc, pollen mother cell; ta, tapetum; v, vacuole. Scale bars = 0.5 mm (**a**), 50 µm (**b**), 0.8 mm (**c**), 20 µm (**d**), 15 µm (**e**), 10 µm (**f**, **h**), 5 µm (**g**), and 2.5 µm (**i**), 1 µm (**j**)

PA, USA), for 48 h. Semithin Sects. (120–200 nm) for LM were collected in glass slides, stained with toluidine blue (2,5% in water) for 5 min, rinsed in distilled water, and air-dried. The sections were permanently mounted in Entellan®. The sections were then analyzed, and digital images were obtained using an upright microscope (Axioskop 2 photomicroscope, Carl Zeiss, Jena, Germany). For TEM analyses, ultrathin Sects. (60–90 nm) were obtained using a diamond knife in an ultramicrotome (Porter Blum MT2, Dupont-Sorvall), collected on copper grids (300 mesh), and poststained with aqueous uranyl acetate (2.5%), followed by lead citrate (0.1%) (Reynolds 1963). Sections were examined at 80 kV under a transmission electron microscope (JEM1400 JEOL, Tokyo, Japan), and the images were digitalized. For light microscopy (LM), explants were fixed in a modified Karnovsky solution for 1 h under vacuum at room temperature. The fixative was refreshed, and after 36 h without vacuum, the samples were dehydrated through an ethanol series (from 10 to 100% v/v). Samples were embedded in Historesin (Leica). Semi-thin sections of 5 µm, were obtained and stained with 0.05% toluidine blue. Results were photo-documented using a Zeiss Axioskop 2 HBO 100 w/2 or Zeiss Axiophot. Fresh dissected flower, anthers and pistils were observed with a Zeiss Discovery V8 stereomicroscope and photo-documented using a Zeiss AxioCam MRc.

In vitro culture of anthers—an assay to observe changes in microspore development

Inflorescence of *B. brizantha*, BRA 002,747, and *B. decumbens*, BRA 004430, were collected from the field. Racemes were excised and surface sterilized by immersion in 70% ethanol, for 5 min, followed by immersion in a commercial bleach solution (2.5% active chlorine), for 20 min. The racemes were then rinsed three times with autoclaved water. *B. brizantha* stage 8 anthers were isolated and inoculated in Petri dishes containing YP medium supplemented with the antiauxin 2,3,5-triiodobenzoic acid, TIBA 0.2 µM, and activated charcoal, at pH 5.8 (Genovesi 1990). Three Petri dishes with 20 anthers per dish were prepared. Cultures were maintained in a growth chamber at 25 ± 1 °C, in the dark, for 75 days. Anthers were subcultured every 30 days. Anthers of *B. decumbens* at a stage equivalent to stage 7 were placed in liquid N6 medium (Chu 1978) pH 5.8, with a total of 50 anthers per Petri dish and three Petri dishes.

Histology of *B. brizantha* cultivated anthers

To characterize microspore development, anthers were collected at 45 and 75 days, fixed in a solution of 2% glutaraldehyde, 2% paraformaldehyde, 0.001 M $CaCl_2$ in 0.2 M sodium cacodylate buffer, pH 7.2, for 1 h under vacuum at room temperature followed by 36 h at 4 °C. The samples were then dehydrated in an ethanol series (35 to 100%) and embedded in Historesin (Leica) and polymerized at room temperature. Histological Sects. (5 µm) were obtained using a rotary microtome (Leica RM2155); stained with 0.05% toluidine blue in water and mounted using Entellan® (Merck). The analysis was performed in the light microscope Zeiss Axioskop2 HBO 100 w/2 and digital images were obtained.

Localization of SERK transcripts in cultivated anthers of *B. decumbens*

In situ hybridization (ISH) was performed as described by Dusi (2015) and Koehler et al. (2020). Briefly, anthers of *B. decumbens* at the stage equivalent to stage 8 were collected and fixed overnight in 4% paraformaldehyde and 0.25% glutaraldehyde in phosphate buffer, at pH 7.2. Thereafter, they were rinsed, dehydrated in an ethanol series, and infiltrated in butyl methyl methacrylate (BMM). Sections of 0.4 µm were obtained and deposited on glass slides. After BMM removal, tissues were used for ISH. *Bbriz*SERK sense and antisense probes labeled with digoxigenin, were prepared according to Koehler et al. (2020), and used at a final concentration of 0.6 ng/µL hybridization solution. ISH was performed overnight at 42 °C. After rinsing, blocking, and immunodetection typical violet precipitation, indicating hybridization, was observed under a light microscope with differential interference contrast (DIC).

Results

Stages of anther development analyzed using light (LM) and transmission electron microscopy (TEM)

The hermaphrodite flower of *Brachiaria* has three stamens, one pistil with one ovary and two styles with an

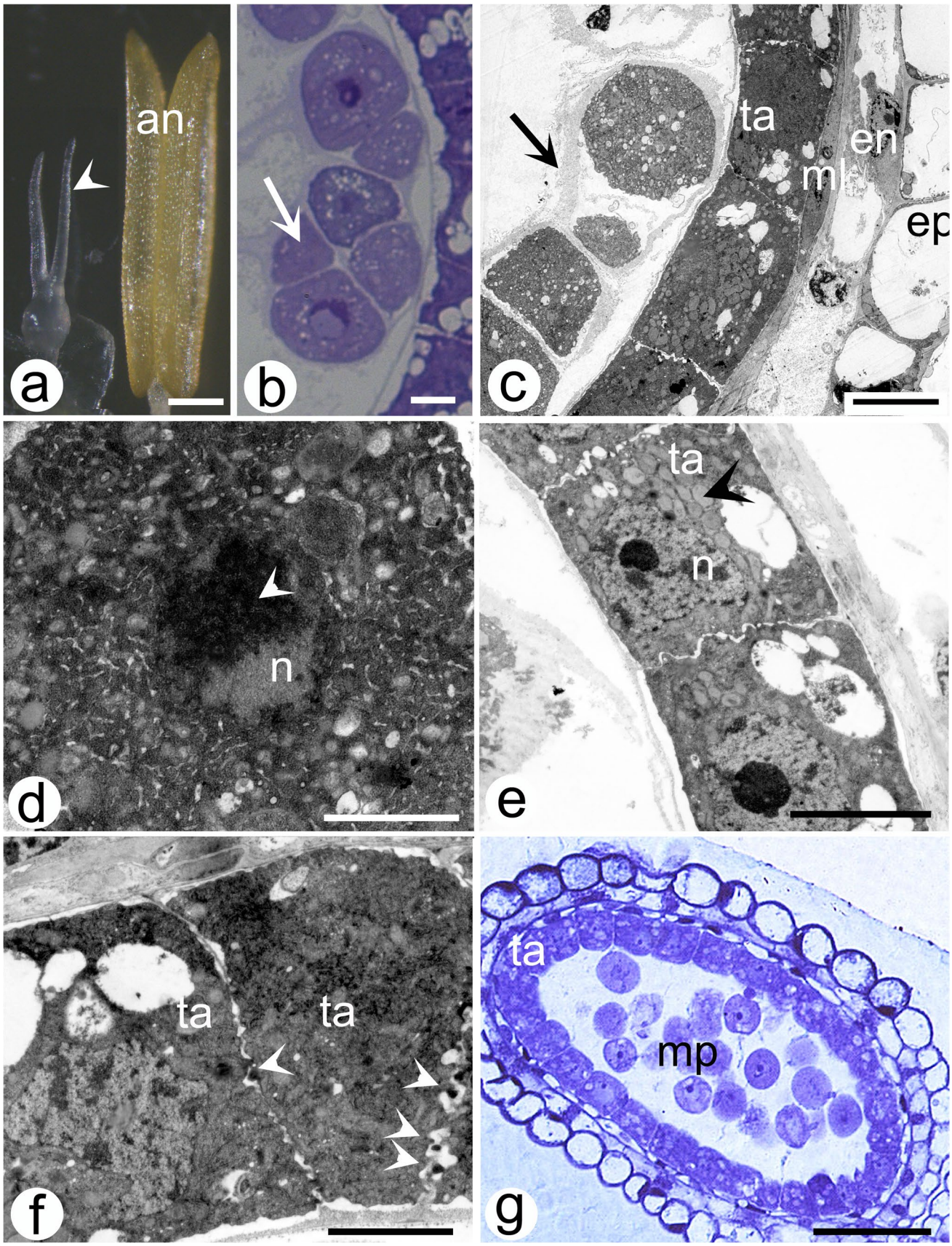
an
a
b
ta
en
ml
ep
c
n
d
ta
n
e
ta
ta
f
ta
mp
g

◂**Fig. 3** Anther development in *B. brizantha*, stage 5. **a–b**, **g** LM images, **c–f** TEM images. **a** Pistil and anther at stage 5 showing stylodium (arrow). **b** Tetrad of microspores (arrow). **c** Anther wall layers and degrading callose wall surrounding microspores of the tetrad (arrow), near the tapetum. Note the highly vacuolated epidermis and endothecium and the very thin middle layer. **d** Detail of a microspore from the tetrad showing condensed chromatin. **e** Tapetum cells showing a lobated nucleus and prominent nucleolus (arrow) and lipid bodies (arrowhead). **f** Detail of tapetum cells, note a number of initial Ubisch bodies secreted by the tapetum cells (white arrowheads). **g** Free microspores. Abbreviations: an, anther; en, endothecium; ep, epidermis; ml, middle layer; mp, microspores; n, nucleus; pp, plastids; ta, tapetum; te, tetrads. Scale bars = 0.3 mm (**a**), 5 µm (**b**, **c**, **e**, **f**), 2 µm (**d**) and 50 µm (**g**)

enlarged feathery stigma. This stigma can cover a large part of the style and is also called a stylodium (Fig. 1a). From the observation of the archesporial cells to the anther opening, 11 stages are distinguished with the following characteristics:

Stage 1 represents the beginning of anther development, when the spikelets are very tender, with well-developed glumes, lemma, and palea. The translucent anther (Fig. 1b) shows bilateral symmetry. In the cross section, the epidermis has elongated cells with anticlinal divisions. The differentiation of the thecae and the delimitation of the locules are not yet visible. Subepidermally, the archespore cell is distinguished (Fig. 1c). When the spikelets reach 1 to 2 mm in length, in elongating anthers (Fig. 1d), the connective tissue differentiates the vascular tissue joining the four defined locules (Fig. 1e). The anther wall is composed of the epidermis with a visible cuticle and the outer and the inner subepidermal layers; centrally in the locule, the sporogenous cells differentiate and enlarge (Fig. 1f). All cells present a dense cytoplasm. The ultrastructure of the parietal and sporogenous cells are comparable in cytoplasmic density and vacuolation; mitochondria/plastids are more evident in the sporogenous cell (Fig. 1g, h). At stage 3, hermaphrodite flowers are approximately 1 mm in length and contain small pistils with a very short style and stylodium, with anthers exhibiting a pale green color (Fig. 2a). The anther wall is fully formed with four layers of cells: epidermis, endothecium, middle layer, and tapetum (Fig. 2b). Inside the locule, in stage 4, prominent nucleus and nucleolus are found in pollen mother cells (Fig. 2c, d), with yellow translucent anthers, and callose start to be deposited around the cells from the center of the anther locule (Fig. 2e), preceding the first meiotic division (Fig. 2f, g). Highly vacuolated cells are observed, especially in the epidermis, endothecium, and middle layer, while tapetum cells have smaller vacuoles (Fig. 2h). At this stage, the tapetum cells present a conspicuous nucleus and a prominent nucleolus (Fig. 2i) and plasmodesmatal connections are observed between tapetum cells (Fig. 2j). After meiosis, the important tetrad period follows when callose envelopes every microspore and the entire tetrad. When pale-yellow anthers are approximately 2.5 mm in length, the pistil has an elongated stylodial axis (Fig. 3a), at stage 5, marked by the late tetrad stage (Fig. 3b, c, d), with the dissolution of the callose wall, the isobilateral tetrad enters a disintegration process (Fig. 3c, d). At this stage, the tapetum cells show electron-dense particles, with a lobate nucleus and prominent nucleolus, cytoplasm with many lipid bodies (Fig. 3e), and initial signs of Ubisch bodies (UB) (Fig. 3f). Finally, the callose disappears and free microspores are released inside the locule (Fig. 3g). Subsequently, at stage 6, anthers are yellow, 3 mm in length, and stigmatic hairs develop in pistils (Fig. 4a). Microspores have migrated toward the anther wall (Fig. 4b, c), some of them observed with the microspore pore against the turgid tapetum cell, which presents a dense cytoplasm. Microspores present exine and small vacuoles (Fig. 4d) and are against the Ubisch bodies secreted by the tapetal cells (Fig. 4e). Finally, the tapetum shows initial signs of degeneration (Fig. 4f). At stage 7, anthers are 3.5 to 4 mm in length; the pistil shows a white feathering-like stylodium with long white hairs (Fig. 4g). At this stage, microspores have a single large vacuole that presses the cytoplasm and the nucleus toward the cell wall (Fig. 4h). A sign of advanced degeneration of the anther wall was observed, tapetum cells have dense cytoplasm, and the middle layer is almost imperceptible (Fig. 4i, j). At stage 8, anthers are 4 to 5 mm in length, and the pistil has elongated red/purple stylodium (Fig. 5a). Starch grains accumulate in the microspores, and the pore develops in the same position (Fig. 5b, c). Anthers finally reach the final length of 5 mm, and the pistil has stylodium with dark hairs at stage 9 (Fig. 5d). A two-locule anther is a result of the septum rupture (Fig. 5e). Microspores divide by mitosis and cytokinesis results in a smaller generative and a larger vegetative cell (Fig. 5f, g). Exine and intine are very well defined (Fig. 5h). Remnants of the tapetum and Ubisch bodies are present in the locule (Fig. 5i). During anthesis (Fig. 6a), at stage 10, anthers have a deep yellow color with a touch of red and a very fragile cell wall, while pistil presents a very dark stylodium. Anther dehiscence has occurred (Fig. 6b) and, with the opening of the stomium (Fig. 6c), mature tricellular pollen grains are present with the vegetative cell and two generative cells (Fig. 6d). The mature pollen grain contains starch and lipids as storage compounds, the exine and intine, as well as the pore, are fully developed (Fig. 6e). The cytoplasm of the vegetative cell has small osmiophilic lipid bodies, and a high number of small vesicles (Fig. 6f). An operculum covers the pollen grain aperture and the annulus surrounding the operculum is elevated (Fig. 6g).

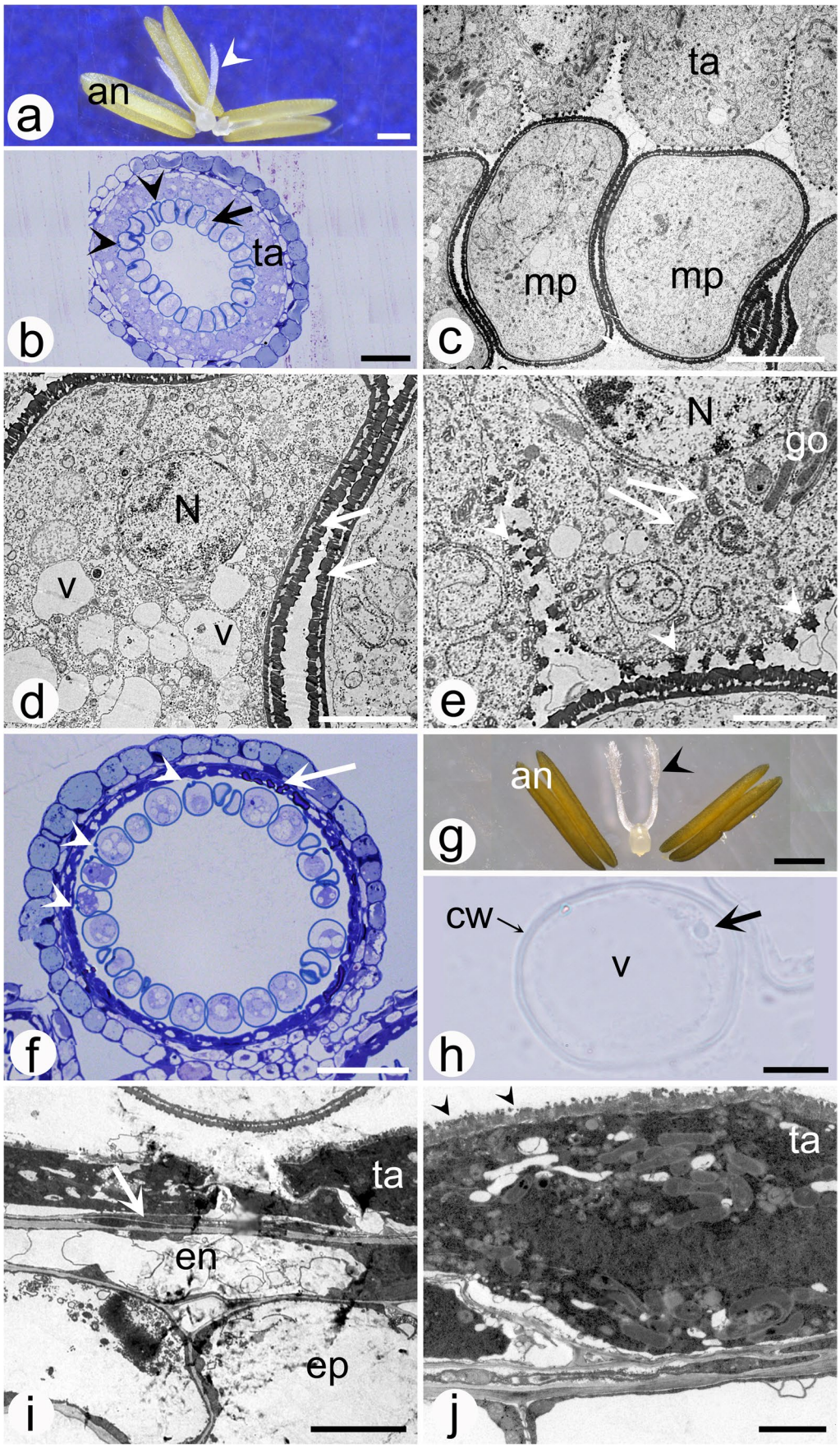
a
an
b
ta
c
ta
mp
mp
d
N
v
v
e
N
go
f
g
an
h
cw
v
i
ta
en
ep
j
ta

◂**Fig. 4** Anther development in *B. brizantha*, stages 6 (**a**–**f**) and 7 (**g**–**j**). **a**, **b**, **f**–**h** LM images, **c**–**e**, **i**–**j** TEM images. **a** Dissected hermaphrodite flower indicating an anther at stage 6 and one stylodium (arrowhead). **b** Microspores organized against the tapetum cells (arrow), some with visible pores (arrowheads) and large tapetum cells. **c** Microspores positioned in contact with the tapetum cells. **d** Detail of the microspore showing small vacuoles and exine. **e** Detail of the tapetum cells next to microspores and Ubisch bodies (arrowheads), which contribute to exine formation. **f** Beginning of tapetum degeneration (arrow), showing microspore pores facing the tapetum (arrowhead); at this stage, the middle cell layer is crushed. **g** Pistil and anthers at stage 8, showing feathered stylodium with long white hairs (arrowhead). **h** Microspores containing a single large vacuole pushing the cytoplasm and nucleus (arrow) toward the cell wall. **i** Degenerating anther wall. Note the middle cell layer crushed (arrow). **j** Detail of a tapetum cell in degeneration still showing Ubisch bodies (arrowheads). Abbreviations: cw, cell wall; en, endothecium; ex, exine; go, Golgi complex; ml, middle layer; mp, microspore; mt, mitochondria; n, nucleus; ta, tapetum; v, vacuole. Scale bars = 0.6 mm (**a**), 40 µm (**b**), 10 µm (**c**, **h**), 3 µm (**d**, **e**), 50 µm (**f**), 1.3 mm (**g**), 5 µm (**i**), and 1 µm (**j**)

The exine is composed of foot layer, baculum, and tectum (Fig. 6h). Finally, at stage 11, the anthers are wilted and empty (Fig. 6i, j). In the dehiscent anther, after pollen grains are released, only two of the four original cell layers remain: the endothecium and epidermis (Fig. 6k).

Table 1 summarizes the characteristics of the 11 cytological stages of sexual *B. brizantha* anther development showing the morphological markers linked to the stages.

Histology of anthers after embryogenesis induction

Stage 8 anthers of sexual *B. brizantha* (Fig. 7a), characterized by mostly late-stage uninucleated microspores with one large vacuole (Fig. 7b), were cultured in YP medium, a medium used originally for maize anther tissue culture (Genovesi 1990). After 30 days in culture, a mass of cells proliferating from the stomium could be seen. Histology of cultured anthers after 75 days in culture showed microspores in equal divisions, with two equally sized nuclei, indicating a possible embryogenic route (Fig. 7c, d, e). Two types of nuclei division were observed. Nuclei side by side in the microspore (Fig. 7c, d), nuclei separated by each other by the vacuole (Fig. 7e). Cytokinesis was not observed. Only in a few cases in anthers cultured for 45 days, multicellular structures could be observed inside the anther locules (Fig. 7f, g).

SERK expression in cultivated anthers of *B. decumbens*

After 30 days in culture, *B. decumbens* anthers presented a mass of cells proliferation from the stomium. At this stage, while *SERK* ISH with the sense probe did not produce a signal (Fig. 7h), hybridization with the antisense probe showed the characteristic ISH signal in some vacuolated microspores (Fig. 7i).

Discussion

Anther development is an essential step of plant reproduction and comprises two phases: the sporophytic and the gametophytic phases. The sporophytic phase includes stamen meristem specification followed by archesporial cells and sporogenous cells formation, differentiation of microsporocytes which undergo meiosis, finishing with the resulting haploid cells, the microspores (microsporogenesis). The gametophytic phase (microgametogenesis), comprises the microspores entering mitosis to produce the microgametophytes, or pollen grains, and their maturation. (Åstrand et al. 2021, Liu et al. 2012, Pandey et al 2022; Scott et al. 2004; Yang et al 2003).

In this work, the development of the anthers from the hermaphrodite flower of *B. brizantha* was categorized in 11 stages that were related to morphological and cytological markers (see Table 1) and *B. brizantha* anther cell wall differentiation, development, and degeneration were closely observed. Anther wall layers play a role during anther development (Ma 2005; Sun et al. 2018). The establishment of the anther wall layers, as we observed in *Brachiaria* sp., followed the pattern of other members of the family Poaceae and other monocots (Gómez et al. 2015; Nakamura et al. 2010). The outer subepidermal layer differentiates into endothecium and the inner subepidermal layer giving rise to the middle layer and the tapetum (Åstrand et al. 2021). In *Brachiaria* sp. this differentiation occurs between stage 2, when the difference between the outer and inner subepidermal layers are obvious, and stage 3 when the four layers of the anther wall are visible is a specialized layer, which functions in the nutrition of meiocytes and microspores (Pacini 2010; Pacini and Franchi 1993; Pacini et al. 1985). Alterations in the pattern of anther wall with the absence of tapetum may result in male sterility (Canales et al. 2002; Walbot and Egger 2016; Yang et al. 2003). In *A. thaliana*, double mutants of *SERK1* and *SERK2*, genes expressed in the tapetum and middle layer precursors, resulted in failures of tapetum specification leading to male sterility (Albrecht et al. 2005; Colcombet et al. 2005). In sexual and apomictic *B. brizantha* genotypes that produce viable pollen, *SERK* expression was observed in PMC and tapetum (Koehler et al. 2020). It is possible that *SERK* genes also play a role in the tapetum specification controlling sporophytic development in *Brachiaria*.

Microsporogenesis phase is marked by the enlargement of tapetum cells and callose deposition in the wall of microsporocytes, initiating from the center of the anther

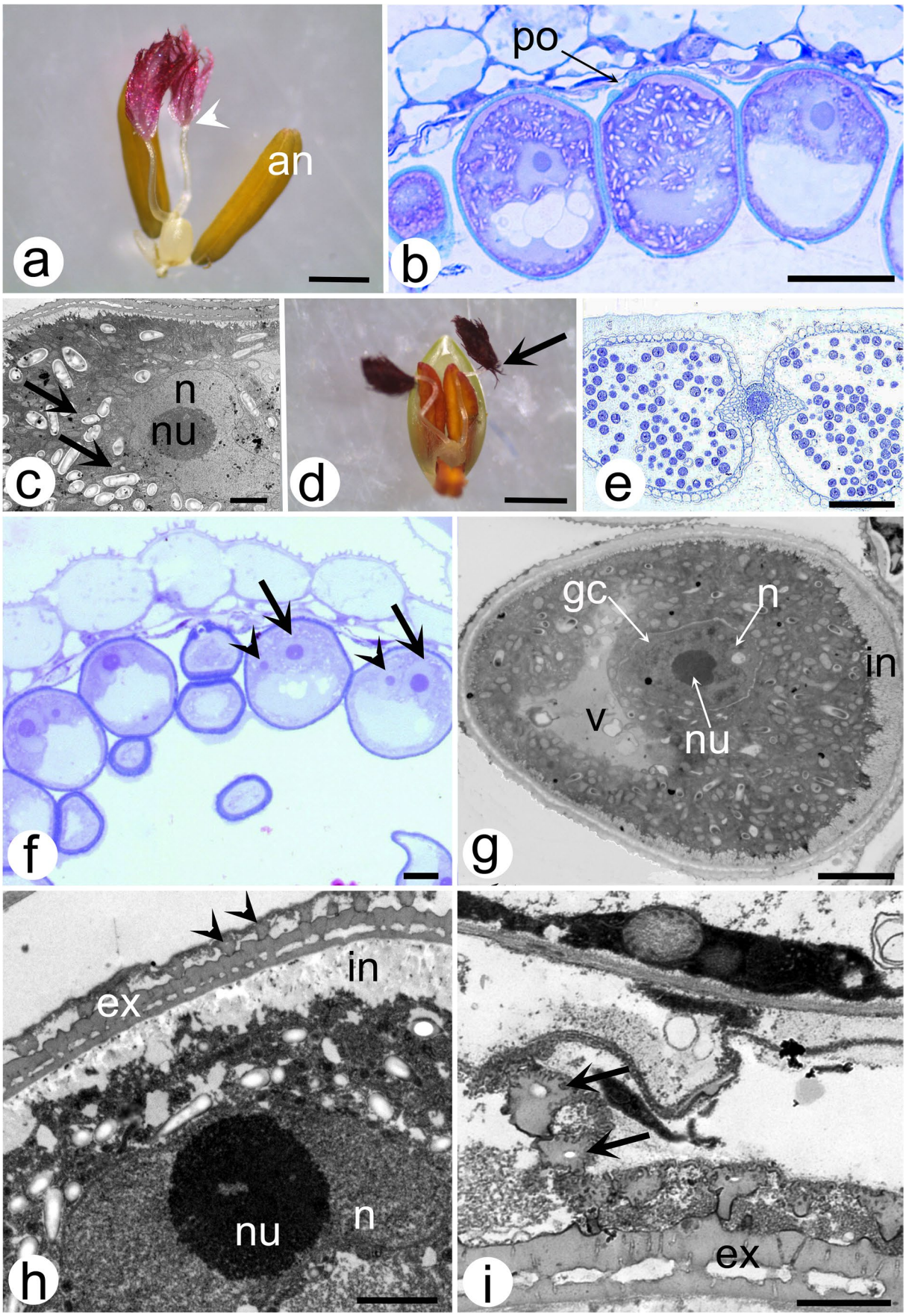
a
an
b
po
c
n
nu
d
e
f
g
gc
n
in
v
nu
h
ex
in
nu
n
i
ex

◂**Fig. 5** Anther development in *B. brizantha*, stages 8 and 9. **a**–**b**, **d**–**f** LM images, **c**, **g**–**i** TEM images. **a–c** Anthers at stage 8 and pistil showing a red stylodium (arrowhead). **b** Microspores are mostly uninucleate and vacuolated, they accumulate starch and the position of the pore remains stable. **c** Detail of the vegetative cell with starch grains in the cytoplasm (arrows). **d** Flower with anther at stage 9, and stylodium with very dark hairs (arrow). **e** The septum rupture results in a two locular anther. **f** Microspores pursue a vegetative (arrow) and a generative (arrowhead) nucleus. **g** Pollen showing the nucleus in the center of the generative cell and a vacuole. **h** The nucleus of the vegetative cell and pollen exine and intine with the Ubisch bodies (arrowheads). **i** Detail of the Ubisch bodies (arrows). Abbreviations: ep, epidermis; ex, exine; GC, generative cell; in, intine; mp, microspores; n, nucleus; nu, nucleolus; po, pore; v, vacuole. Scale bars = 2 mm (**a**), 20 µm (**b**), 5 µm (**c**), 3 mm (**d**), 50 µm (**e**), 10 µm (**f**), 2.5 µm (**g**, **h**), and 0.5 µm (**i**)

locule, similarly to what was observed in *B. decumbens* (Dusi and Willemse 1999a). *B. brizantha*, like other species of Poaceae (Barnes and Blackmore 1992; Pacini 2010) has the parietal type of tapetum. It is attributed to the tapetum, the production of locular fluid, production and secretion of callase, a β-1,3 glucanase. In *Brachiaria* sp., as in other plants, callose digestion led to the release of microspores, ending microsporogenesis.

Microgametogenesis starts at stage 6 up to stage 10 with mature pollen formation. The uninucleate microspore phase starts at the very end of stage 5 and ends at stage 8, a period in which the events of exine and intine formation occur. The pore is visible in the early stages of *B. brizantha* microsporogenesis, a feature also observed in *Brachypodium distachyon* (Sharma et al. 2015a). Meanwhile, microspores migrate toward anther wall, near the tapetum that provides material like. Ubisch bodies (sporopollenin orbicules), for microspore development (Heslop-Harrison and Dickinson 1969). In contrast to what was described for *B. distachyon* (Sharma et al. 2015b), in which Ubisch bodies were observed initially at the free microspore stage, in *B. brizantha*, they were first observed between the tapetum cells at stage 5, when dissolving tetrads were visible. The appearance of the Ubisch bodies secreted from the fully developed tapetum cells toward the microspore wall at stage 6, as observed in this work, is consistent with the exine formation.

Reprogramming microgametogenesis to a sporophytic pathway in *Brachiaria* spp. will benefit from the association of morphological characteristics of anther development in which uninucleate microspores were identified. Aiming embryogenesis in *B. brizantha*, it will be important to establish which one of the anther developmental stages presenting uninucleate microspores, from stage 5 (young microspores) to 8 (microspores entering mitosis), will respond better when culture in vitro. During microspore development, the uninucleate microspore phase is the longer one. Before the inequal division microspores go through structural changes such as a large vacuole formation, nucleus polarization, and exine development. Embryo formation from microspores can follow different pathways, but the competence for embryo induction for most species are the stages just before or after pollen grain mitoses I, as reviewed by Soriano et al. (2013). In some species of the Poaceae family (Silva 2012; Ślusarkiewicz-Jarzina et al. 2017; Maluszynski et al. 2003), microspore embryogenesis is successful when the explants are anthers with uninucleate microspores or the isolated microspores. Taking this into account, in *B. brizantha*, the phase that should be more adequate to androgenesis induction would be amongst the stages 5 to 8. In this work, stage 7 anthers, characterized by vacuolated microspores with one polarized nucleus, were used to evaluate the capacity of their microspores to enter the sporophytic pathway that could result in somatic embryos. While the gametophytic pathway is characterized by inequal divisions, equal divisions could, in some cases, indicate the shift of the gametophytic to sporophytic program characterizing the beginning of the somatic embryogenesis pathway in microspores as observed in species like, *Olea europaeae* L. (Solís et al. 2008) and *Brassica napus* (Zaki and Dickinsonn 1991). In this work, two types of equal binucleate microspores were observed according to the position of a vacuole, a feature that could be related to cytoskeleton rearrangements as observed in *Brassica napus*, in which microtubules rearrangements play a role in microspore equal divisions (Hause et al. 1993). However, for species and genotypes for which information about microspore development in vitro is missing, it is not possible to sustain that symmetrical divisions are a sign of the entrance into an embryogenic route. Actually, there are not enough evidence to confirm that microspores in equal divisions would further develop into embryos (Soriano et al. 2013). In this respect, the detection of *SERK* gene expression in anthers' cultures contributes to establishing if microspores enter an embryogenic route. We previously determined that expression of *SERK* is observed in anthers of *B. brizantha* during microsporogenesis (Koehler et al. 2020) and not during microgametogenesis (data not shown). Here, the expression of *SERK* in uninucleate and equal binucleate microspores of *B. decumbens* observed after 30 days in culture indicates that they are able to enter the embryogenic route. In *B. brizantha*, with few exceptions when multicellular structures were observed, the sporophytic development ceased in the first equal division. Tissue culture conditions have to be optimized to allow the induced microspores to continue the embryogenic route. In addition, other genotypes and stages of anther development should be tested and *SERK* expression can be used to assist experiment evaluation.

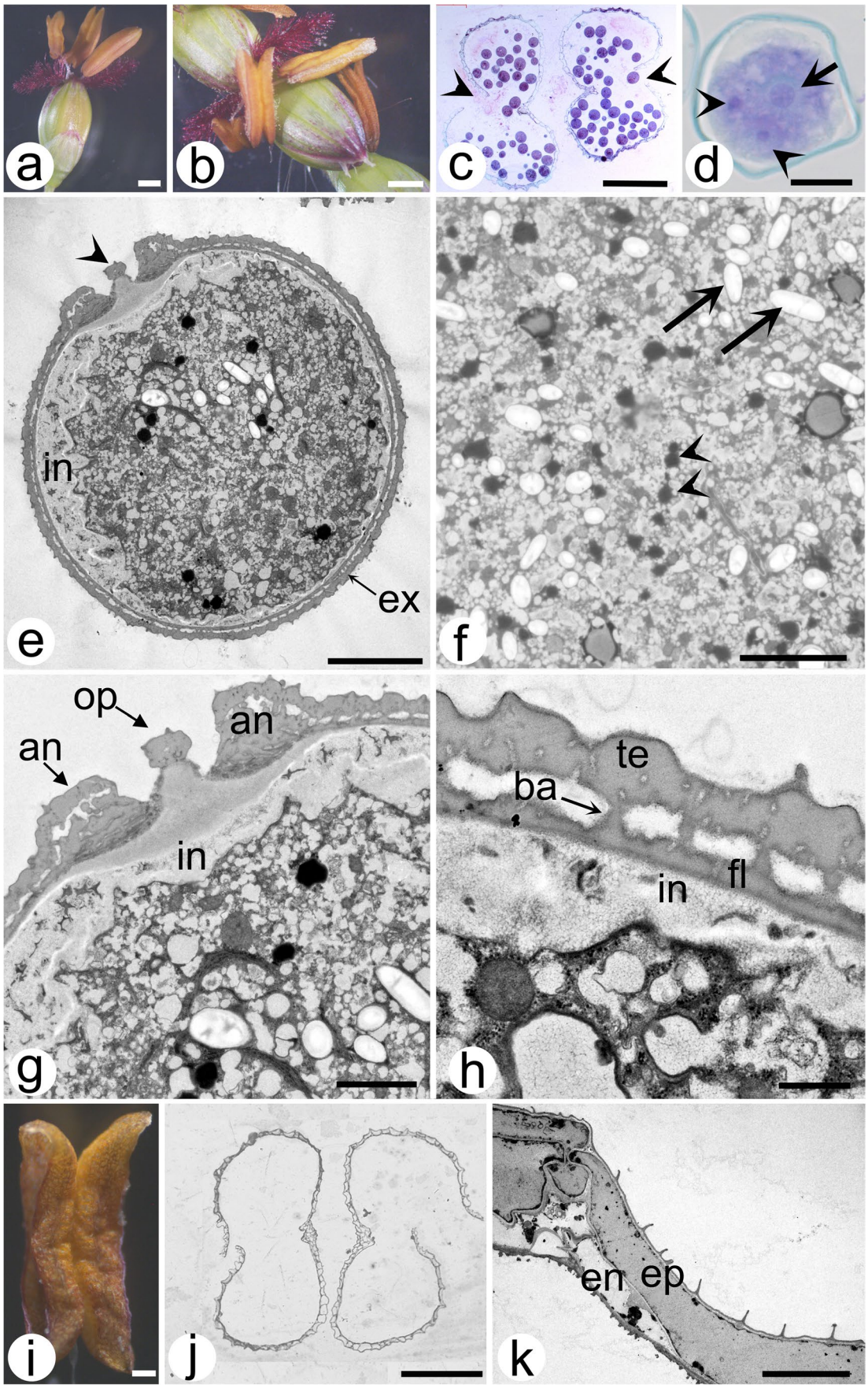
a
b
c
d
in
ex
e
f
op
an
an
in
g
te
ba
in
fl
h
i
j
en
ep
k

◂**Fig. 6** Anther development in *B. brizantha*, stages 10 and 11. **a**–**d**, **i**–**j** LM images, **c**–**f** TEM images. **a**–**b** At anthesis, anthers at stage 10. **c** Section of the apex of the anther showing stomium opening (arrowheads) and releasing the pollen grains. **d** Pollen grain with the generative nucleus (arrow) and two sperm nuclei (arrowhead). **e** Mature pollen grain with starch and lipids, intine and exine, and a well-developed pore (arrowheads). **f** Cytoplasm of the vegetative cell of a mature pollen grain showing small osmiophilic lipid bodies (arrowheads) and small vesicles (arrows). **g** Detail of the elevated annulus surrounding the operculum that covers the aperture. **h** Detail of the pollen wall showing intine and the exine layers, tectum, baculum or columella, and foot layer. **i** Stage 11: wilted and empty anther. **j** Section of apex of the empty anther. Note that the connective tissue is not present. **k** Wall of dehiscent anther after pollen grains release, only two of the original four layers remains: the endothecium and the epidermis. Abbreviations: an, annulus; ba, baculum; en, endothecium; ep, epidermis; ex, exine; fl, foot layer; in, intine; op, operculum; te, tectum. Scale bars = 1 mm (**a**), 2 mm (**b**), 200 µm (**c**, **j**), 10 µm (**d**), 5 µm (**e**), 2 µm (**f**, **g**), and 0.5 µm (**h**, **i**), 10 µm (**k**)

Different approaches have been used to analyze the development of anther and pollen wall (Jaffri and MacAlister 2022; Xue et al. 2021) and pollen development (Gómez-Mena et al. 2022), but morphological markers of the stage of pollen development remain important as a base for further studies (Jaffri and MacAlister 2022). The association of morphological characteristics, identifying the stages to anther and pollen grain or ovule and embryo sac development, is the basis for studying and unrevealing the genes and metabolic pathways involved in the process of reproduction, as known from monocotyledonous such as *B. decumbens* (Dusi and Willemse 1999a, b), *Hordeum vulgare* (Gómez and Wilson 2012), *B. distachyon* (Sharma et al. 2015a, 2015), and *Triticum aestivum* (Browne et al. 2018). Up to now, four stages of pistil morphology have been used as a parameter to isolate anthers of *B. brizantha*. The aspect of the stylodia provides a good marker to establish the stage of anther development due to the evident modification in morphology that occurs during flower growth. The data collected and analyzed here, which defined and characterized 11 stages during anther development, gives a much more precise indication of male development and more than one morphological characteristic might be used to select the stage. In addition to the benefits for haploid culture, molecular studies will profit from the knowledge provided here. *Brachiaria* is an open pollination plant, and breeding could benefit from a male-sterile plant in intraspecific crosses between sexual plants, that went through an artificial polyploidization, and the polyploid apomicts.

Table 1 Events observed during anther development in *Brachiaria brizantha*

	Morphological markers		Microscopical events	
Stages	Anther characteristic	Characteristics of spikelet/flower or pistil stage	Anther	Pollen grain development
1	Translucent	Spikelets with well-developed glumes, one male and one hermaphrodite flower	Bilateral symmetry, epidermis, primary parietal cells	Archesporial cells, primary sporogenous cells
2	Translucent	Young spikelets 1–2 mm	Four locules, connective tissue, outer and inner subepidermal layers	Sporogenous cells
3	Pale green	Hermaphrodite flower ~1 mm. Pistil with very small stylodia	Epidermis, endothecium, middle layer, tapetum	Pollen mother cell
4	Yellow-translucent ~2 mm	Pistil with elongating stylodial axis		Callose wall around pollen mother cell and meiotic division
5	Pale yellow ~2.5 mm	Pistil with elongating stylodial axis		Tetrads disintegration, free microspores, first sign of Ubisch bodies
6	Yellow ~3 mm	Pistil with stylodia hairs	Degenerated middle layer, first signs of tapetum degeneration	Microspores with small vacuoles organized near the anther wall, visible pore, exine formation
7	Yellow ~3.5–4 mm	Pistil with long stylodia and stigmatic hairs		Microspores with only one vacuole, polarization of the nucleus
8	Yellow ~4–5 mm	Stylodium is completely elongated and hairs become tinted red		Starch accumulation, intine deposition
9	Yellow, swollen (very fragile wall) ~5 mm	Stylodium with dark hairs totally red	Rupture of the septum resulting in anther with two locules	
10	Yellow, swollen (very fragile wall) ~5 mm	Stylodium with red hairs	Anthesis, dehiscence of anthers. Stomium breakage and beginning of pollen release	Mature tricellular pollen,
11	Wilted anthers	Stylodium with dark red hairs	Epidermis	Pollen grains released

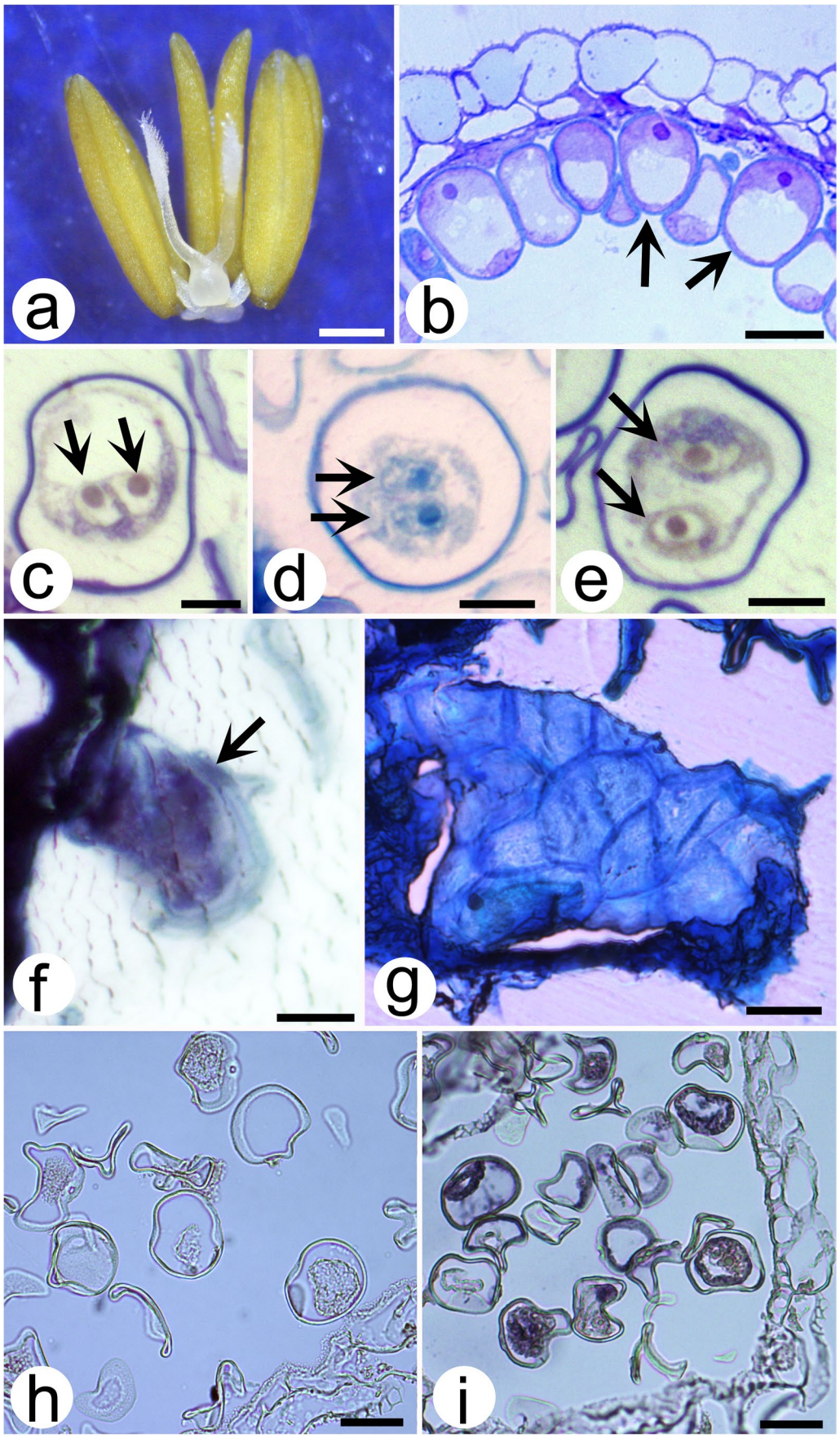
a
b
c
d
e
f
g
h
i

◂**Fig. 7** Flower with anthers at stage 7 of *B. brizantha*. **a** Dissected flower showing stage 3 pistil and the three anthers at stage 8. **b** Transverse section of the anther at stage 8 with the microspores with a single nucleus and a large vacuole (arrows). **c–e** Binucleate microspores after mitosis without cytokinesis, from 75 days cultured anthers, stained with toluidine blue, with two equally sized nuclei (arrows). **f–g** Multicellular structures inside the locules in anthers after 45 days in culture. **h–i** In situ hybridization in sections of anther cultured for 30 days with sense probe (**h**) without hybridization signal, and with the antisense probe (**i**) showing high signal in vacuolated microspores and binucleate microspores after mitosis. Scale bars = 1 mm (**a**), 25 µm (**b**), 10 µm (**c–f**), and 20 µm (**g–i**)

Conclusions

The dynamics of the in vivo development of sporophytic tissues and gametophytic cells of *B. brizantha* was described in this work by morphological and cytological analyses, reaching our objective. This work provides a rapid assessment of the stages of anther and pollen development in *B. brizantha,* using as markers the length of spikelet, hermaphrodite flower, length, and coloration of anthers, and pistil morphology. It can be used to direct cellular and molecular studies that rely on specific stages of anther development, such as pollen embryogenesis, haploid and double haploid production, identification of genes related to the events of anther development. The detailed morphological and cytological characterization of 11 stages of development presented here adds important knowledge to *B. brizantha* reproductive development and complements the information presented in the reproductive calendar of *B. decumbens* (Dusi and Willemse 1999a). This is a guideline for *Brachiaria* sp. for anther and pollen development to find the suitable stage for haploid cell culture.

Acknowledgements The authors acknowledge Prof. Dr. Michiel T.M. Willemse for critically reviewing the manuscript; Conselho Nacional de Desenvolvimento Científico e Tecnológico, (CNPq) for the doctorate scholarship (141959/2006-1) for ADK and Research Fellowship for APM (305785/2008-7); Empresa Brasileira de Pesquisa Agropecuária (Embrapa) for financial support; Coordenação de Aperfeiçoamento de Pessoal de Nível Superior – Brasil (CAPES) – Finance Code 001. We cordially acknowledge CMI-FOP-UNICAMP coordinated by Prof. Pedro D. Novaes for the use of the transmission electron microscope.

Author contribution ADK, APM, VTCC, and DMAD designed the project; ADK, MLR, DMAD, and GBC performed experimental procedures; ADK, MLR, DMAD, VTCC, and APM performed image analysis; ADK, MLR, GBC, VTCC APM, and DMAD participated in the research, analyzed the data, and wrote the article. All authors read and approved the final manuscript.

Funding Empresa Brasileira de Pesquisa Agropecuária, Coordenação de Aperfeiçoamento de Pessoal de Nível Superior, 001, Adriana Martinelli, Conselho Nacional de Desenvolvimento Científico e Tecnológico 141959/2006-1, Andréa Koehler, 305785/2008-7, Adriana Martinelli.

Declarations

Competing interests The authors declare no competing interests.

References

Albrecht C, Russinova E, Hecht V, Baaijens E, De Vries S (2005) The *Arabidopsis thaliana* somatic embryogenesis receptor-like kinases1 and 2 Control Male Sporogenesis. Plant Cell 17:3337–3349

Alves ER, Carneiro VTC, Araujo ACG (2001) Direct evidence of pseudogamy in an apomictic *Brachiaria brizantha* (Poaceae). Sex Plant Rep 14:207–212. https://doi.org/10.1007/s00497-001-0120-6

Alves ER, Carneiro VTC, Dusi DMA (2007) In situ localization of three cDNA sequences associated with the later stages of aposporic embryo sac development of *Brachiaria brizantha*. Protoplasma 231:161–171. https://doi.org/10.1007/s00709-007-0253-z

Araujo ACG, Nóbrega JM, Pozzobon MT, Carneiro VTC (2005) Evidence of sexuality in induced tetraploids of *Brachiaria brizantha* (Poaceae) Euphytica 144:39–50

Åstrand J, Knight C, Robson J, Talle B, Wilson ZA (2021) Evolution and diversity of the angiosperm anther: trends in function and development. Plant Rep 34:307–319. https://doi.org/10.1007/s00497-021-00416-1

Barnes SH, Blackmore S (1992) Ultrastructural organization of two tapetal types in angiosperms. Arch Histol Cytol 55:217–224

Browne RG, Iacuone S, Li SF, Dolferus R, Parish RW (2018) Anther morphological development and stage determination in *Triticum aestivum*. Front Plant Sci 9:1–13. https://doi.org/10.3389/fpls.2018.00228

Canales C, Bhatt AM, Scott R, Dickinson H (2002) EXS, a Putative LRR receptor kinase, regulates male germline cell number and tapetal identity and promotes seed development in Arabidopsis. Curr Biol 12:1718–1727

Chu, C.C. (1978) The N6 medium and its applications to anther culture of cereal crops. In: Proceedings of Symposium on Plant Tissue Culture, Science Press, Peking, pp 45–50.

Colcombet J, Boisson-Dernier A, Ros-Palau R, Vera CE, Schroeder JI (2005) *Arabidopsis* somatic embryogenesis receptor kinases1 and 2 are essential for tapetum development and microspore maturation. Plant Cell 17:3350–3361

Dusi DMA (2001) Apomixis in *Brachiaria decumbens* Stapf. PhD thesis, University of Wageningen, Wageningen

Dusi DMA (2015) Hibridização in situ para detecção da expressão de genes em tecidos vegetais. In: Brasileiro ACM, Carneiro VTC (eds) Manual de transformação genética de plantas, 2nd edn. Embrapa, Brasilia, pp 303–327

Dusi DMA, Willemse MTM (1999a) Apomixis in *Brachiaria decumbens* Stapf.: gametophytic development and reproductive calendar. Acta Biol Cracov Ser Bot 41:151–162

Dusi DMA, Willemse MTM (1999b) Activity and localisation of sucrose synthase and invertase in ovules of sexual and apomictic *Brachiaria decumbens*. Protoplasma 208:173–185

Dusi DMA, Alves ER, Willemse MTM, Falcão R, Valle CB, Carneiro VTC (2010) Toward in vitro fertilization in *Brachiaria* spp. Sex Plant Reprod 23:187–197. https://doi.org/10.1007/s00497-010-0134-z

Genovesi AD (1990) Maize (*Zea mays* L.): In vitro production of haploids. In: Bajaj YPS (ed) Biotechnology in agriculture and forestry, vol. 12: Haploids in crop improvement I. Springer-Verlag Berlin Heidelberg, pp 176–203

Gómez JF, Talle B, Wilson ZA (2015) Anther and pollen development: a conserved development pathway. J Integr Plant Biol 57(11):876–891

Gómez JF, Wilson ZA (2012) Non-destructive staging of barley reproductive development for molecular analysis based upon external morphology. J Exp Bot 63:4085–4094. https://doi.org/10.1093/jxb/ers092

Gómez-Mena C, Honys D, Datla R, Testillano PS (2022) Editorial: advances in pollen research: biology, biotechnology and plant breeding applications. Front Plant Sci 13:876502. https://doi.org/10.3389/fpls.2022.876502

Guimarães LA, Dusi DMA, Masiero S, Resentini F, Gomes ACMM, Silveira ED, Florentino LH, Rodrigues JCM, Colombo L, Carneiro VTC (2013) *BbrizAGL6* is differentially expressed during embryo sac formation of apomictic and sexual *Brachiaria brizantha* plants. Plant Mol Biol Rep 31:1397–1406. https://doi.org/10.1007/s11105-013-0618-8

Hause B, Hause G, Pechan P, Van Lammeren AAM (1993) Cytoskeletal changes and induction of embryogenesis in microspore and pollen cultures of *Brassica napus* L. Cell Biol Int 17:153–168

Heslop-Harrison J (1982) Pollen-stigma interaction and cross-incompatibility in the grasses. Science 215(4538):1358–1364. https://doi.org/10.1126/science.215.4538.1358

Heslop-Harrison J, Dickinson HG (1969) Time relationships of sporopollenin synthesis associated with tapetum and microspores in *Lilium*. Planta 84:199–214

Jaffri SRF, MacAlister CA (2022) Sequetial deposition and remodeling of cell wall polymers during tomato pollen development. Front Plant Sci 12:703713. https://doi.org/10.3389/fpls.2021.703713

Junqueira Filho RG, Mendes-Bonato AB, Pagliarini MS, Bione NC, Borges do Valle C, de Oliveira Penteado MI, (2003) Absence of microspore polarity, symmetric divisions and pollen cell fate in *Brachiaria decumbens* (Gramineae). Genome 46:83–8. https://doi.org/10.1139/g02-114

Koehler AD, Irsigler AST, Carneiro VTC, Cabral GB, Rodrigues JCM, Gomes ACMM, Togawa RC, Costa MMC, Martinelli AP, Dusi DMA (2020) SERK genes identification and expression analysis during somatic embryogenesis and sporogenesis of sexual and apomictic Brachiaria brizantha (syn. Urochloa brizantha). Planta 252:39. https://doi.org/10.1007/s00425-020-03443-w

Lacerda ALM, Dusi DMA, Alves ER, Rodrigues JCM, Gomes ACMM, Carneiro VTC (2012) Expression analyzes of *Brachiaria brizantha* genes encoding ribosomal proteins *BbrizRPS8*, *BbrizRPS15a* and *BbrizRPL41* during development of ovaries and anthers. Protoplasma 250:505–514. https://doi.org/10.1007/s00709-012-0433-3

Ma H (2005) Molecular genetic analyses of microsporogenesis and microgametogenesis in flowering plants. Annu Rev Plant Biol 56:393–434. https://doi.org/10.1146/annurev.arplant.55.031903.141717

Maluszynski M, Kasha KJ, Foster BP, Szarejko I (2003) Doubled haploid production in crop plants. Springer, Dordrecht. https://doi.org/10.1007/978-94-017-1293-4

Mendes-Bonato AB, Pagliarini MS, Forli F, Valle CB, Penteado MIO (2002) Chromosome numbers and microsporogenesis in *Brachiaria brizantha* (Gramineae). Euphytica 125:419–425

Mendes-Bonato AB, Felismino MF, Kaneshima AMS, Pessim C, Calisto V, Pagliarini MS, Valle CB (2009) Abnormal meiosis in tetraploid genotypes of *Brachiaria brizantha* (Poaceae) induced by colchicine: its implications for breeding. J Appl Genet 50:83–87. https://doi.org/10.1007/BF03195658

Miles JW, Valle CB (1996) Manipulation of apomixis in *Brachiaria* breeding. In: Miles JW, Maass BL, Valle CB (eds) *Brachiaria*: Biology, agronomy and improvement. Ciat, Cali-Colombia, pp 164–177

Monteiro LC, Verzignassi JR, Barrios SCL, Valle CB, Fernandes CD, Benteo GL, Libório CB (2016) Characterization and selection of interspecific hybrids of *Brachiaria decumbens* for seed production in Campo Grande - MS. Crop Breed Appl Biot 16:174–218. https://doi.org/10.1590/1984-70332016v16n3a27

Nakamura AT, Longhi-Wagner HM (2010) Scatena VL (2010) Anther and pollen development in some species of Poaceae (Poales) Braz. J Biol 70(2):351–360

Ndikumana J (1985) Etude de l'hybridation entre espèces apomictiques et sexuées dans le genre *Brachiaria*. Ph.D. thesis, Université Catholique de Louvain, Belgium

Nogler GA (1984) Gametophytic apomixis. In: Johri BM (ed) Embriology of angiosperms. Springer-Verlag, Berlin, pp 475–518

Pacini E (2010) Relationships between tapetum, loculus, and pollen during development. Int J Plant Sci 171:1–11

Pacini E, Franchi GG (1993) Role of the tapetum in pollen and spore dispersal In: Hesse M, Pacini E, Willemse MTM (eds) The Tapetum: cytology, function, biochemistry and evolution. Plant systematics and evolution (Supplementum 7). Springer-Verlag, Vienna, p 1–11

Pacini E, Franchi GG, Hesse M (1985) The tapetum: its form, function, and possible phylogeny in *Embryophyta*. Pl Syst Evol 149:155–185

Pandey S, Moradi AB, Dovzhenko O, Touraev A, Palme F, Welsch R (2022) Molecular control of sporophyte-gametophyte ontogeny and transition in plants. Front Plant Sci 12:789789. https://doi.org/10.3389/fpls.2021.789789

Risso-Pascotto C, Pagliarini MS, Valle CB (2006) Microsporogenesis in *Brachiaria dictyoneura* (Fig. & De Not.) Stapf (Poaceae: Paniceae). Genet Mol Res 5:837–845

Rodrigues JCM, Cabral GB, Dusi DMA, Mello LV, Rigden DJ, Carneiro VTC (2003) Identification of differentially expressed cDNA sequences in ovaries of sexual and apomictic plants of *Brachiaria brizantha*. Plant Mol Biol 53:745–757

Scott RJ, Spielman M, Dickinson HG (2004) Stamen structure and function. Plant Cell 16:S46–S60. https://doi.org/10.1105/tpc.017012

Sharma A, Singh MB, Bhalla PL (2015a) Anther ontogeny in *Brachypodium distachyon*. Protoplasma 252:439–450. https://doi.org/10.1007/s00709-014-0689-x

Sharma A, Singh MB, Bhalla PL (2015b) Ultrastructure of microsporogenesis and microgametogenesis in *Brachypodium distachyon*. Protoplasma 252:1575–1586. https://doi.org/10.1007/s00709-015-0793-6

Solís M-T, Pintos B, Prado M-J, Bueno M-Á, Raska I, Risueno M-C, Testillano PS (2008) Early markers of *in vitro* microspore reprogramming to embryogenesis in olive (*Olea europaea* L.). Plant Sci 174:597–605

Soriano M, Li H (2013) Boutilier K (2013) Microspore embryogenesis: establishment of embryo identity and pattern in culture. Plant Reprod 26:181–196. https://doi.org/10.1007/s00497-013-0226-7

Silva TD (2012) Microspore Embryogenesis. In: Sato, K-I (ed), Embryogenesis, pp 573–596. https://doi.org/10.5772/37039

Silveira ED, Guimarães LA, Dusi DMA, Silva FR, Martins NF, Costa MMC, Alves-Ferreira M, Carneiro VTC (2012) Expressed sequence-tag analysis of ovaries of *Brachiaria brizantha* reveals genes associated with the early steps of embryo sac differentiation of apomictic plants. Plant Cell Rep 31:403–416. https://doi.org/10.1007/s00299-011-1175-y

Skerman PJ, Riveros F (1989). Tropical grasses. FAO Plant production and protection series 23, FAO, Rome

Ślusarkiewicz-Jarzina A, Pudelska H, Woźna J, Pniewski T (2017) Improved production of doubled haploids of winter and spring triticale hybrids via combination of colchicine treatments on anthers and regenerated plants. J Appl Genetics 58:287–295. https://doi.org/10.1007/s13353-016-0387-9

Spurr AR (1969) A low-viscosity epoxy resin embedding medium for electron microscopy. J Ultra Struct R 26:31–43

Sun L, Xiang X, Yang Z, Yu P, Wen X, Wang H, Abbas A, Khan RH, Zhang Y, Cheng S, Cao L (2018) *OsGPAT3* plays a critical role in anther wall programmed cell death and pollen development in rice. Int J Mol Sci 19:4017. https://doi.org/10.3390/ijms19124017

Valle CB, Jank L, Resende RMS (2009) O melhoramento de forrageiras tropicais no Brasil. Revista Ceres 56:460–472

Walbot V, Egger RL (2016) Pre-meiotic anther development: cell fate specification and differentiation. Annu Rev Pant Biol 67:365–395

Weyen J. (2021) Applications of doubled haploids in plant breeding and applied research. In: Segui-Simarro J.M. (eds) Doubled Haploid Technology. Methods in Molecular Biology, vol 2287. Humana, New York, NY. https://doi.org/10.1007/978-1-0716-1315-3_2

Worthington M, Heffelfinger C, Bernal D, Zapata YP, Quintero C, Perez JG, Vega JD, Miles J, Dellaporta J, Tohme J (2016) A parthenogenesis gene candidate and evidence for segmental allopolyploidy in apomictic *Brachiaria decumbens*. Genetics 203:1117–1132. https://doi.org/10.1534/genetics.116.190314

Xue J-S, Yao C, Xu Q-L, Sui C-X, Jia X-L, Hu W-J, Lv Y-L, Feng Y-F, Peng Y-J, Shen S-Y, Yang N-Y, Lou Y-X, Yang Z-N (2021) Development of the middle layer in the anther of *Arabidopsis*. Front Plant Sci 12:634114. https://doi.org/10.3389/fpls.2021.634114

Yang S-L, Xie L-F, Mao H-Z, Puah CS, Yang W-C, Jiang L, Sundaresan V, Ye D (2003) *TAPETUM DETERMINANT1* is required for cell specialization in the *Arabidopsis* anther. Plant Cell 15:2792–2804. https://doi.org/10.1105/tpc.016618

Zaki M, Dickinson H (1991) Microspore-derived embryos in *Brassica*: the significance of division symmetry in pollen mitosis I to embryogenic development. Sex Plant Reprod 4:48–55